Acta Cryst. (1987). B43, 64-71

Crystal Form and Surface Morphology of Modulated β-K_2SO_4-Type Structures

BY B. DAM* AND P. BENNEMA

RIM, Laboratory of Solid State Chemistry, Faculty of Science, Catholic University of Nijmegen, Toernooiveld, NL-6525 ED Nijmegen, The Netherlands

(*Received* 6 *March* 1986; *accepted* 31 *July* 1986)

Abstract

The morphological consequences of a displacive modulation of the $[(CH_3)_4N]_2ZnCl_4$ crystal structure are investigated. The morphology can be divided into a main part, relatively unperturbed by the properties of the modulation wave, and the so-called satellite morphology. On the main faces, the surface morphology appears to remain unaffected by the successive changes of the modulation wave vector with temperature. Optical goniometry suggests a continuous orientation change of the satellite faces with respect to the main morphology upon a change of the modulation wave vector **q**. The corresponding surface morphological changes have been studied by *in situ* optical microscopy. The satellite $(10\bar{1}2)$ surface behaves as a flat *F* face. The stabilization of certain step trains by the modulation wave is considered to be responsible for this *F*-face behaviour.

1. Introduction

In the study of crystal form attention has gradually shifted from the crystal bulk structure to an analysis of the crystal surface structure. On the one hand surface reconstruction has been extensively studied (Weeks & Gilmer, 1979), whereas on the other hand attention has been focused on the roughening of the solid-liquid interface (Mönch, 1979). The 3D crystal structure is still of utmost importance for the crystal form. In principle, the crystal form allows the determination of the dimensionless unit-cell constants and, in fortuitous cases, even of the crystal space group. In the history of classical morphology the influence of superstructures on the crystal form has been almost totally neglected. This may partly be due to the fact that satellite reflections were interpreted in terms of a superstructure at a time when classical morphological crystallography was already starting to be out of fashion (Dehlinger, 1927).

In 1980, a four-index approach to the description of the morphology of the so-called modulated structures was introduced (Janner, Rasing, Bennema & van der Linden, 1980). This paper was followed by two others, showing the innate connection between the length and symmetry of periodic structural-displacement waves and crystal form (Dam & Janner, 1983, 1986). In the one-dimensional modulated case the modulation wave vector $\mathbf{q} = \alpha\mathbf{a}^* + \beta\mathbf{b}^* + \gamma\mathbf{c}^*$ can be added as a fourth basic vector to the three reciprocal basic vectors of the undistorted unit cell: $\mathbf{a}^*, \mathbf{b}^*, \mathbf{c}^*$. Then the crystal faces can be indicated by the integers (*hklm*), the indices of the new face normals $\mathbf{k} = h\mathbf{a}^* + k\mathbf{b}^* + l\mathbf{c}^* + m\mathbf{q}$.

The four-index method for describing the morphology of modulated crystals corresponds to the four indices defining the diffraction pattern of incommensurate crystals, which lead to the superspace approach introduced for these substances by de Wolff (1977), Janner & Janssen (1980) and Janner (1983). The wave vectors **k** describing the Fourier density waves of a one-dimensional modulated crystal can be expressed as *integral* linear combinations of (3 + 1) basic vectors. The same basic vectors of course are used in our morphological description and the indices *hklm* indicate the wave vectors of the Fourier matter density wavefronts parallel to the crystal-face surface. Irrespective of the fact of whether the length of **q** fits with the basic lattice or not (the commensurate and the incommensurate cases respectively), crystal faces of modulated structures can thus be indicated by *four low integers*.

The main faces (*hkl*0) whose orientation is not affected by the appearance of a structural modulation, can be distinguished from the satellite faces (*hklm*), $m \neq 0$. The latter are only present in modulated crystal phases and change in orientation with respect to (*hkl*0) upon any change of **q**. If **q** changes continuously with temperature (as is often the case in incommensurate phases) a continuous orientational change of the (*hklm*) faces is to be expected.

Such continuous behaviour would be clearly in conflict with present theories on the stability of crystal faces such as the periodic bond chain (PBC) (Hartman, 1973) and connected net analyses (Rijpkema, Knops, Bennema & van der Eerden, 1982), currently used to describe the stability of normal main faces. Even the Bravais concept of the morphological importance (MI) of lattice planes with a higher reticular density is completely lost. The question then arises whether satellite faces should be considered to

* Present address: Philips Research Laboratories, PO Box 80 000, 5600 ZA Eindhoven, The Netherlands.

0108-7681/87/010064-08$01.50

be fundamentally different from main faces. Do satellite faces differ from *F* faces which are defined as faces with a roughening temperature larger than 0 K, *i.e.* with a non-zero edge free energy (see *e.g.* van der Eerden, Bennema & Cherepanova, 1978)?

These questions on the nature of satellite faces have been studied by *in situ* microscopy. In the first preliminary communication on the surface morphology of satellite faces (Dam, 1985) we have already reported the occurrence of growth spirals, etch pits and so-called hollow cores on the $(10\bar{1}2)$ satellite face of $[(CH_3)_4N]_2ZnCl_4$ (here denoted as TMA-ZC) in its commensurate and incommensurate phases. Thus it was suggested that in each phase, commensurate or incommensurate, the edge free energy on this satellite face is larger than zero. Secondly, at the commensurate–commensurate phase transition characterized by an abrupt change of **q** from $2/5\mathbf{c}^*$ to $1/3\mathbf{c}^*$, the roughening of the corresponding $(10\bar{1}2)$ satellite orientation was observed. Although the bonding nature of the satellite faces is still unclear, these observations support the idea that they do indeed behave as stable *F*-face orientations.

In this article we intend to give an overview of the morphological consequences of structural modulations for modulated K_2SO_4-type structures, concentrating mainly on TMA-ZC. First we will show that the position of a satellite face on $[(CH_3)_4N]_2ZnCl_4$ can be monitored as a function of temperature. The results suggest a *continuous orientational change*. Secondly, surface-morphological features on both main faces and the $(10\bar{1}2)$ satellite face will be analysed. A qualitative model for the stability of the satellite faces will be given. The derivation of laws governing the appearance of satellite faces may also be important in deriving a perturbative approach to the morphology of complicated crystal structures.

2. Structure and crystal form

2.1. *Modulated β-K_2SO_4-type structures*

Previously, several satellite faces have been identified on Rb_2ZnBr_4 (Janner, Rasing, Bennema & van der Linden, 1980), called RZB here, and TMA-ZC (Dam & Janner, 1986) single-crystalline spheres, which had been grown at the temperatures of their modulated phases.

These modulated structures essentially have the same basic β-K_2SO_4-type structure in common. Superposed on the undistorted structure (spacegroup *Pcmn*) is a displacive modulation with a wave vector $\mathbf{q} = \gamma\mathbf{c}^*$. This wave vector attains several commensurate and incommensurate values.

In RZB **q** is incommensurate ($\gamma = 0{\cdot}29$) for $T <$ 355 K before it locks in to $\gamma = 1/3$ at $T = 193$ K, the ferroelectric commensurate phase (Pater & van Dijk, 1978).

Table 1. *The various phases of* $[(CH_3)_4N]_2ZnCl_4$ *between* 273 *and* 303 K (*Tanisaki & Mashiyama*, 1980; *Almairac, Ribet, Ribet & Bziouet*, 1980)

The wave vector **q** is taken along the pseudo-hexagonal **c** axis, the polarization along the shortest axis **b**.

The various phases of $[(CH_3)_4N]_2ZnCl_4$			
IV	III	II	I
$q = 1/3c^*$	$q = 2/5c^*$	$q \simeq 0{\cdot}42c^*$	para
$T > 181$ K	$T > 276{\cdot}5$ K	$T > 279$ K	$T > 293$ K
$P112_1/n$	$Pc2_1n$	?	*Pcmn*

In TMA-ZC the sequence is more complicated. Up to six modulated phases have been identified. Most important are the first three modulated phases immediately below the para phase, see Table 1. It has been shown (Dam & Janner, 1986) that the morphology in all these four phases can be described by one superspace group $Pcmn(1s\bar{1})$ [see de Wolff, Janssen & Janner (1981) for 4D groups and their extinction conditions]. This group consistently describes both the commensurate phases and the incommensurate phase in one supergroup-group framework. Even phase IV, though monoclinic, still has a pseudo-orthorhombic lattice. The deviation of γ from 90° is very small [$\gamma = 90{\cdot}1$ at $T = 263$ K (Tanisaki & Mashiyama, 1980)] and can be seen as symmetry breaking, the superspace group requiring an orthorhombic lattice which is not imposed by any of the elements of the 3D space group. In particular, the superspace group mentioned above predicts an extinction condition ($h0lm$; $m = 2n$) which is not required by any of the 3D groups describing the commensurate superstructures. This extinction condition was actually found in the TMA-ZC morphology (Dam & Janner, 1986).

It was also shown that the morphology of TMA-ZC can be separated into main and satellite parts. The main part was found to be hardly affected by the modulation wave in any of the three observed modulated phases (II–IV). In contrast, the temperature dependence of the orientation and the morphological importance (MI) of the six identified satellite faces were in good agreement with the known dependence of **q** on *T*. In general the MI of the satellite faces is smaller than the MI of main faces. The satellite orientations manifest themselves as weak but distinct reflections, usually only observable with an optical goniometer.

The incommensurate diffraction pattern of TMA-ZC is characterized by a continuous shift in position of the satellite diffraction spots with respect to the main spots as a function of temperature. This reflects a continuous change in the length of the modulation wave λ, the distance between main and satellite spots being equivalent to $\mathbf{q} = \gamma\mathbf{c}^*$.

In the following sections we concentrate on the orientational behaviour of the strongest satellite face

$(10\bar{1}2)$. The temperature dependence of the modulation wavelength is found to result in an orientational shift of the satellite face. In § 3 the corresponding changes in the surface morphology of both the $(10\bar{1}2)$ and some main $(hkl0)$ faces will be analysed.

2.2. *Morphological determination of* γ

2.2.1. *Experimental procedure.* The orientation of the $(10\bar{1}2)$ satellite face as a function of temperature has been measured as follows. A large single crystal of about $2\times1\times1$ cm was grown in the para phase at 303 K from a supersaturated, slightly acidified solution. Then a crystal slice, cut approximately along $(10\bar{1}2)$ and polished with a soft slightly wetted tissue, was grown for about one day in a thermostatted, slightly supersaturated solution at temperatures ranging from 298 to 274 K. During growth the initially polished crystal surface develops into small isles of satellite faces partly bounded by strong main faces. The orientation of the satellite face can then be measured quite accurately with respect to these main faces by optical goniometry. Only when the slice is grown at low supersaturation is a sharp reflection obtained.

This method is more accurate than growing crystalline spheres, which on the other hand has the advantage that in principle all crystal orientations get an equal chance to develop. Using a crystal slice one, so to speak, encourages a certain direction to develop and the goniometer reflection of an orientation parallel to the slice improves accordingly. In principle, orientations can be obtained within 10′; in practice, given the quality of the satellite surface, one obtains angles within ±20′; the reproduciblity also lies within these limits.

2.2.2. *Results.* As in our case $\mathbf{q}=\gamma\mathbf{c}^*$, the relation between φ (the angle between [001] and $[h0lm]$) and $\mathbf{q}$ is simply given by:

$$\tan\varphi = ha^*/(l+m\gamma)c^* \qquad (1)$$

Below 298 K the first weak $(10\bar{1}2)$ satellite reflection was measured. The intensity of the reflection increases gradually upon lowering the temperature. In Fig. 1 the morphologically obtained values for γ are plotted. The plot is quite comparable with the X-ray and neutron studies of Almairac, Ribet, Ribet & Bziouet (1980) and Marion, Almairac, Lefebvre & Ribet (1981) respectively. Two plateaus of constant γ can be discerned at $\gamma=1/3$ and $\gamma=2/5$. Our transition temperatures and values for γ deviate somewhat from theirs but this is not uncommon for this class of compounds and is generally ascribed to the effects of defects and impurities (Mashiyama, Tanisaki & Hamano, 1982). The transition temperatures, which are found to lie around 279 and 277 K respectively, cannot be determined with higher accuracy as the optical reflection is not sharp at the transition.

The error bars indicated correspond to the maximum angular spread of ±20′. It is clear that the incommensurate satellite orientation differs significantly from that corresponding to $\gamma=2/5$. In addition significant orientational shifts can be observed *within* the incommensurate $\gamma=2/5$ phase, suggesting a continuous behaviour of the satellite orientation.

The surface orientation was found to resist fast temperature changes. The equilibrium orientation is obtained only after a growth time of about 12–24 h.

This extraordinary behaviour of the satellite face once more stresses that, in addition to the lattice periodicity, the periodicity of a displacive modulation also plays an important role in crystal morphology. Note that the amplitude of such a modulation wave typically lies in the range 0·1–0·5 Å (Hogervorst, 1983).

To gain a deeper insight into what happens structurally at the crystal surface during these phase transitions, we will now turn to the surface morphology of modulated crystals.

3. Surface morphology

3.1. *Experimental procedure*

The *in situ* experiments were performed with an Olympus Vanox optical reflection microscope using oblique illumination and conventional optics. The apparatus has been described before (Jetten, van der Hoek & van Enckevort, 1983) and follows from the methods introduced by Tsukamoto (1983), Tsukamoto & Sungawa (1985) and van Enckevort (1984).

For the study of the main $(hkl0)$ surfaces, large as-grown crystals were used. In order to study the microscopic behaviour of the TMA-ZC $(10\bar{1}2)$ satellite surfaces, crystal plates were again sawn from a large single crystal grown at 303 K. The slice, roughly oriented along $(10\bar{1}2)$, was placed in a thermostatted stagnant solution growth cell (Dam, Polman & van Enckevort, 1984). Close to the crystal surface the temperature of the solution was measured with a plastic-coated thermocouple. The microscope image

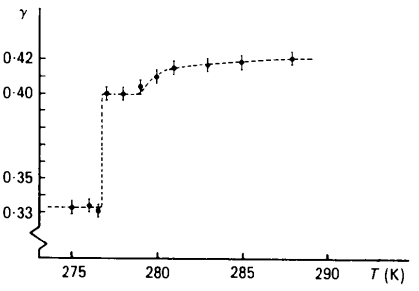

Fig. 1. Morphological determination of the temperature dependence of the TMA-ZC wave vector $\mathbf{q}=\gamma\mathbf{c}^*$, as measured by optical goniometry.

was recorded on video tape using an analog contrast amplifier. With this system step heights of the order of 100 Å can be observed (Dam & van Enckevort, 1984).

3.2. *Surface morphology of the main* $[(CH_3)_4N]_2ZnCl_4$ *faces*

As remarked above in the section on crystal form, the morphological importance (MI) of the TMA-ZC main faces (*hkl*0) remains relatively unperturbed at the advent of structural modulations. By definition the distance between equivalent lattice planes, $d_{(hkl0)} = \mathbf{k}^{-1}$, is not affected by a change of $\mathbf{q}$. Structurally, the only change on superstructure formation is the increase of the surface area of the 2D unit mesh of these main faces. In the incommensurate case it is of course impossible to speak of a unit mesh: it is infinite.

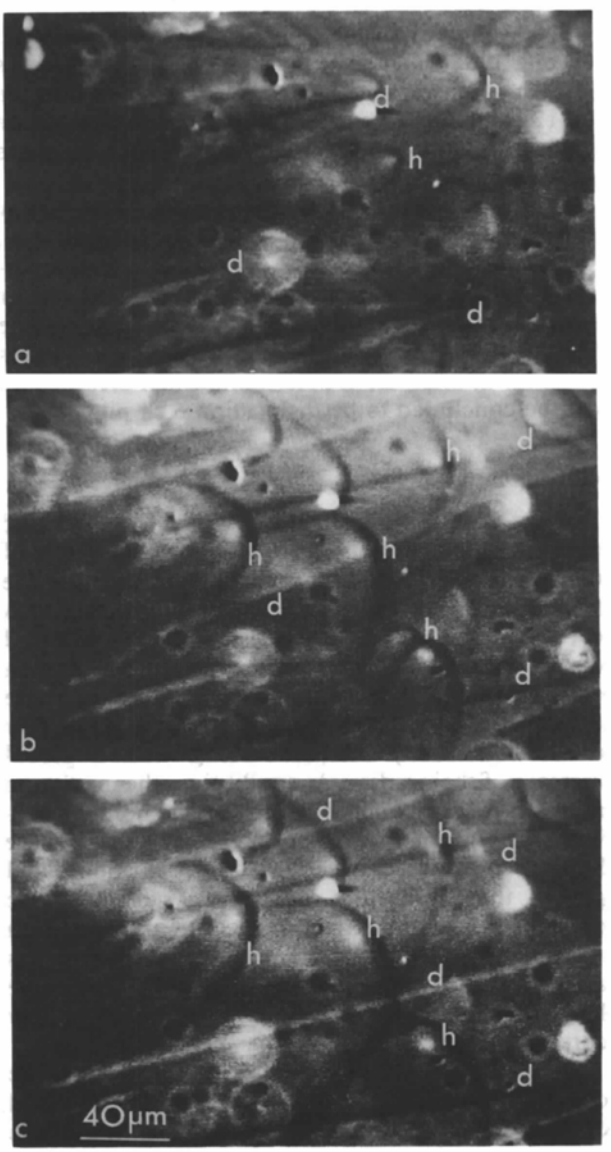

Fig. 2. Surface effects of monoclinic domain formation observed on TMA-ZC (0100) between 276·5 and 276 K using *in situ* optical microscopy. (*a*) Domain walls (d) proceeding from left to right; (*b*) roof-type surface structure develops; (*c*) stable configuration after rearrangement. Growth hillocks (h) are also indicated.

It was still disappointing, however, to find in our microscopical investigation that even the crystal surfaces of the main faces do not reveal any effects that can be related to the modulation wave. Examining the (0010), (1010), (2010), (1000), (1100), (1110) and (0100) faces, circular growth spirals and etch pits were found but nothing happened to them at the phase transitions; no change in step height, step distance or step kinetics was observed, not even on (0010). This face has a dual character as it is normal to the modulation wave vector and can also be seen as a satellite face (0001).

The only interesting effect observed is not due to the modulation wave but rather to the symmetry breaking in phase IV. On all but the faces lying in the [010] zone we observed what we deduce to be the effect of monoclinic domain formation. At $T \simeq 276{\cdot}4$ K lines are suddenly formed which divide the surface into parallel strips of 20–50 μm. As the crystal transforms to the monoclinic phase at this temperature, we suspect these strips to be the macroscopic result of changes of the unit-cell parameters at this transition. Upon monoclinic transformation at least two types of domains will be formed with a monoclinic angle $\gamma = 90 \pm 0{\cdot}1$. Presuming a reorientation of the *b* axis, all surfaces not lying in the [010] zone will break up in a kind of roof-type structure. Hence the observed lines must be twin boundaries dividing different surface inclinations corresponding to two types of domains. In Fig. 2 the successive stages of this process are shown. Twin boundaries oriented parallel to **c** advance from left to right and after rearrangement divide the surface into strips of inclined surfaces. A small hysteresis was observed as the lines only disappeared when increasing the temperature to 276·8 K. At the transition the twin planes become very mobile and the surface transforms back to its initial flatness.

Step advancement was not found to be hindered by this break up of the crystal surface.

Monoclinic domain formation in this phase was observed earlier by Mashiyama, Hasebe & Tanisaki (1980) using polarization microscopy. They found domain walls both parallel to *a*–*c* and *b*–*c*. This seems to be at variance with our observations. The first results of our own polarization microscopy study however indicate that close to the transition temperature (down to 275 K) only *b*–*c* domains are formed.

A surface feature that we could not quite interpret is the occurrence of large holes of about 5–10 μm in diameter. Their radius is not very sensitive to the

supersaturation and, in contrast to our observations on the main (2010) surface of Rb_2ZnCl_4, they did not emit spiral steps.

3.3. *Surface morphology of the* (2010) *main face of* Rb_2ZnCl_4

The main faces of Rb_2ZnCl_4 (RZC) were also investigated in our *in situ* study. This compound is isostructural with RZB. Incommensurability sets in below $T = 302$ K while the ferroelectric 1/3 phase is reached at $T = 192$ K (Sawada, Shiroishi, Yamamoto, Takashige & Matsuo, 1977). Although RZC appeared to be less suitable for *in situ* studies than TMA-ZC, one feature on (2010) was too impressive to remain unmentioned.

On the (2010) surface very large holes were observed, again with a typical diameter of 5–10 μm. In contrast to those observed on TMA-ZC, some of these holes were found to emit strongly bunched growth spirals, see Fig. 3. Moreover, the radius of the hollow core could be decreased (or increased) somewhat by increasing (or decreasing) the supersaturation. Obviously one would interpret such a phenomenon as a hollow core and its growth spiral, which may develop around dislocations as described by Cabrera & Levine (1956). Such hollow cores are not commonly observed on inorganic salts, however, as their typical equilibrium radius should be at least one or two orders of magnitude smaller.

In one case, in which the supersaturation was slowly increased, the hollow core collapsed suddenly instead of the slow closing down one would expect. The core was filled, while the spiral kept rotating as before. Dislocation splitting could be a possible cause for this effect. Only edge-type dislocations should have bent away, otherwise a change in the spiral behaviour would be expected. It is more likely that this hollow core was a metastable one probably formed upon the closing of an inclusion. An X-ray diffraction-stress birefringence study on alum (van Enckevort & Odekerken, 1982) beautifully demonstrated the relation between hollow tubes followed by series of inclusions and the dislocation line connecting them.

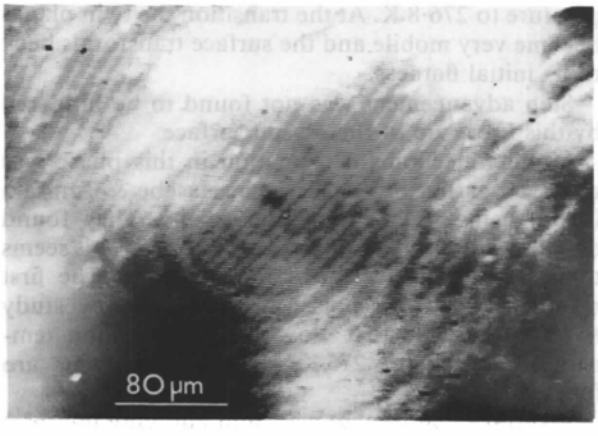

Fig. 3. Metastable hollow core emitting bunched growth spiral on (2010) Rb_2ZnCl_4; *in situ* optical microscopy.

In conclusion, we note that no evidence was found either on TMA-ZC or on RZC main faces to identify the observed holes with *stable* hollow cores.

4. Surface morphology of the $[(CH_3)_4N]_2ZnCl_4$ $(10\bar{1}2)$ satellite face

4.1. *Growth spirals and etch pits*

It has already been reported in a preceding letter (Dam, 1985) that in all three modulated phases growth spirals and etch pits can be observed on the $(10\bar{1}2)$ satellite face. Here, we intend to treat the surface morphology of this satellite face in more detail.

The growth spirals become especially visible at low supersaturation, appearing in a strongly bunched, slowly rotating fashion. This bunching at low supersaturation might be an impurity effect as at higher supersaturation the bunches loose coherency while their rotation increases enormously. The etch pits obtained at dissolution persist on further etching and can be concluded to be dislocation etch pits.

4.2. *Stable hollow cores*

Apart from the observation of layer growth and etch pits, which both indicate the *F*-face character of the satellite surface, it is worthwhile to mention the frequent occurrence of large *stable* hollow cores. A correspondence exists between these holes observed during growth and the pits formed around them upon etching. In Fig. 4 these holes can be seen as white dots. Upon lowering the supersaturation the number of dots gradually increases along with a global increase of their radius. At equilibrium the maximum radius is reached and upon etching the hollow cores immediately open up to form the etch pits. These hollow cores were found in all three modulated phases, the equilibrium radius always being of the order of 5 μm. In contrast to the holes observed on the main faces, in this case no irreversible effects appeared and we believe the holes to be real stable hollow cores. Nevertheless, none of these hollow cores was seen to emit growth steps.

According to recently developed theories on the occurrence of stable hollow cores by the stress field of dislocations (van der Hoek, van der Eerden & Bennema, 1982; van der Hoek, van der Eerden, Bennema & Sunagawa, 1982), the radius of a hollow core r_{hc} is generally given by:

$$r_{hc} = r_0 f(\Delta\mu/kT) \qquad (2)$$

The function $f(\Delta\mu/kT)$ is a monotonically decreasing function of the driving force of crystallization, where $\Delta\mu$ is the difference between the chemical potential of the solute and the solid particles. Regarding the temperature dependence we see that our hollow cores behave as they should according to (2). Assuming for the moment that equation (2) is valid for this situation and keeping in mind that the stable hollow cores are only found on the satellite surface and not on any of the main surfaces, we will discuss two causes for the anomalously large value of the hollow core radius:

(*a*) Anomalous behaviour of the stress field of the dislocations emerging at this surface.

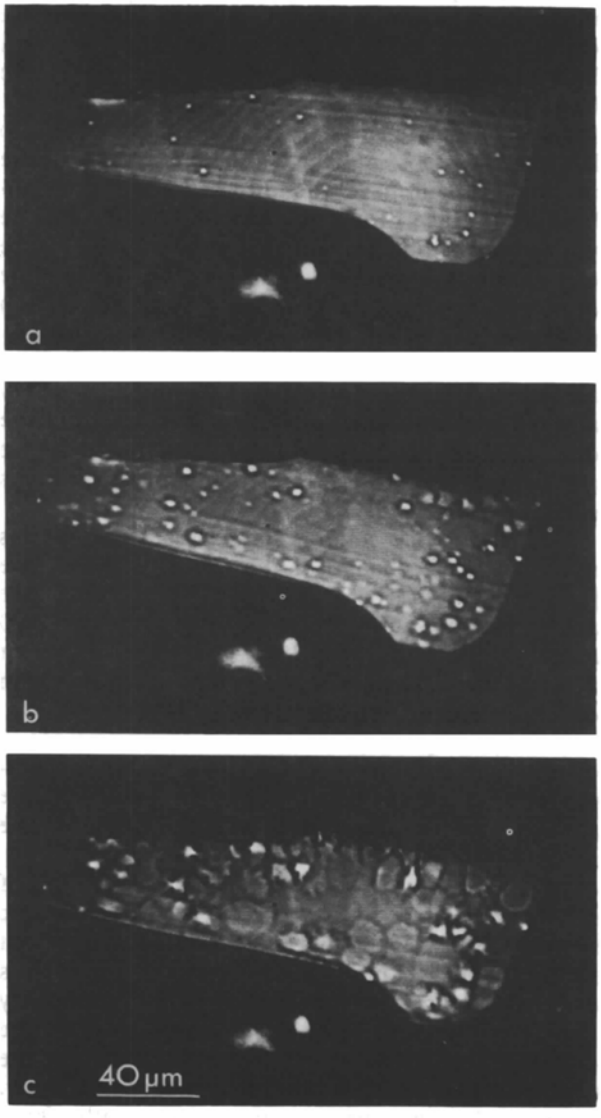

Fig. 4. Sequence showing stable hollow-core formation on the $(10\bar{1}2)$ face of TMA-ZC. (*a*) Growth spiral and some hollow cores; (*b*) approaching equilibrium: more hollow cores and an increase in radius; (*c*) etch-pit formation during dissolution; *in situ* optical microscopy.

(*b*) Extremely low edge free energy of the satellite surface.

Nothing is yet known about the strain fields of dislocations in incommensurate crystals. Only one Lang-topographic investigation has been published on the defect structure of TMA-ZC (Ribet, 1983). However, nothing was reported on the changes in the Burgers vector of the disolcations with the onset of the modulation. One easily figures that for those *e.g.* with a Burgers vector parallel to $\mathbf{k}(hkl0)$ (excluding the case that $\mathbf{b}\|\mathbf{q}$) an extra stress term should be added. Although the length of such a Burgers vector does not depend on $\mathbf{q}$, a phase shift of the modulation wave has to be accounted for. This is due to the phase jump of the modulation wave at the junction between the different lattice planes connected by the Burgers vector. Burgers vectors along a $\mathbf{k}(hklm)$ suffer both from an increase in layer thickness (and hence of Burgers vector length) *and* from a phase shift. Hence dislocations with an extremely large stress field cannot be excluded.

Regarding point (*b*), the edge free energy of a satellite face must certainly be low. This is indicated by the fact that the morphological importance of these faces is very low on TMA-ZC. Moreover, the disappearance of satellite faces at higher supersaturation is probably due to kinetical roughening, which is only possible when the equilibrium edge free energy is low. Thus, we cannot exclude either of the two. The study of the properties of dislocations in TMA-ZC and the study of the kinetical roughening on $(10\bar{1}2)$ is a very promising tool for gaining a deeper understanding of the structural nature of the satellite surfaces.

4.3. *Phase transitions*

4.3.1. *The* III–IV *transition.* In the preceding letter (Dam, 1985) we concentrated on the surface effects at the III–IV transition. A roughening transition was observed. Contrary to the normal sense in which this term is used, the roughening reported there was not due to a temperature effect but resulted from a change in structure. The structural change makes the old satellite orientation unstable in the new phase. From the coexistence of rough and flat surface parts, we concluded the transition to be of first-order character. As the features of the transition were seen to depend strongly on the surface involved, we suggested a surface phase transition triggered by the changes in the bulk structure.

At the II–III transition the orientational changes are not so dramatic and more subtle effects are to be expected. Here we will show that the surface morphology of the $(10\bar{1}2)$ face might give a clue to the continuous adjustment to the modulation wavelength.

4.3.2. *The* II–III *transition.* At the incommensurate–commensurate II–III transition no dramatic surface

changes were found. In fact we could not distinguish between changes within the incommensurate phase and the phase transition itself. Very often however straight lines parallel to [010], *i.e.* normal to **q**, were observed, especially in the incommensurate phase. Such lines can be seen vaguely on Fig. 4 and are more pronounced on Fig. 5. These lines were formed in particular at a change of temperature. They gradually develop, but are hardly ever seen to move. The spiral steps pass them as if they are thick immobile bunches. The nature of these bunches was not immediately clear, they were found both in the incommensurate as well as in the commensurate 2/5 phase. Their thickness seemed to depend only on the temperature changes applied. To check the influence of any bulk effects we partly dissolved the bunched surface. On the etched surface no lines were observed. Only after regrowing the surface did the lines reappear, though at different positions. The only way to remove the lines was to keep the temperature stable or to grow and observe the crystal slice only in the commensurate 2/5 phase. In the latter case, only a few lines are formed which are not affected by temperature changes as long as one stays within the commensurate phase.

Combining our observations on the behaviour of these lines with the orientational changes plotted in Fig. 1, we conclude that the bunches may serve to accommodate steps which have become superfluous at an orientational change of the satellite surface. Such behaviour would be in accordance with a 'stabilized-step' model describing the stability of satellite faces.

The stability of interacting stepped configurations, initially discussed by Landau (1965), has received increased attention lately. Normally, stepped orientations are not thermodynamically stable and have a roughening temperature $T_c = 0$ K. Various authors (Rottman & Wortis, 1984; Schulz, 1985) have now shown that weak step–step interactions lead to substantial increases of the roughening temperatures T_c for whole families of stepped configurations.

Some of these orientations can possibly profit from an interference with the periodicity of the modulation wavelength, assuming that the step free energy will become a function of the step position on the surface plane. Thus, for $\mathbf{q} = \gamma \mathbf{c}^*$ a stepped (100) surface will be more stable for orientations formed by a regular array of steps along **c** with a spacing of $1/\mathbf{q}$.

Imagine now what will happen at a change of **q**. Steps will have to rearrange until they have found their new equilibrium positions with respect to the modulation wave. However, at first the average orientation of the facet is conserved and there will be an excess of steps. The excess of step energy can be reduced in two ways: either the steps reach the facet edge and form an *F* face, or they merge into large macrosteps on the satellite surface. These macrosteps will have the orientation of a neighbouring *F* face. Their relative immobility can be understood if one realizes that such a main *F*-face orientation is of course less rough than the satellite orientation and might even need some nucleation mechanism to proceed over the satellite crystal surface. It remains difficult to imagine how spiral steps are able to pass the macrosteps without being visibly affected and how these spiral steps differ from the ones constituting the macrosteps. Experimentally we are limited here by the fact that monolayer steps cannot be observed.

Calculating the number of excess steps in this model at a 30′ change of the $(10\bar{1}2)$ satellite face [assuming this to be a stepped (100) surface], one arrives roughly at an excess of three steps per 1000 ledge positions. Hence, 300 Å bunches spaced at 10 μm distances are expected, which corresponds in order of magnitude to our observations.

Note that the bunches can be considered as a kind of discommensuration (McMillan, 1976), accommodating a phase shift to keep the other satellite surface parts in accordance with the phase of the modulation wave.

In conclusion, we remark that the observation of satellite faces and the stability of their microscopic surface features is the first indication up to now that subtle displacive modulations manifest themselves even at the crystal surface. Crystal morphology appears to be very sensitive to periodicities in the crystal structure; the morphology is not limited to the three periodicities of the ordinary space lattice only. In particular, the surface structure of satellite faces deserves further investigation.

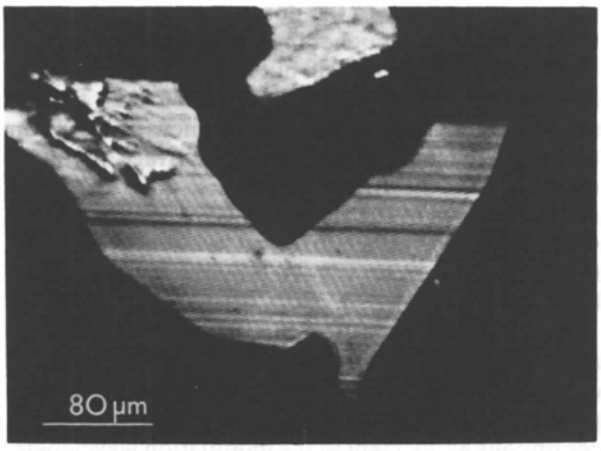

Fig. 5. Immobile bunches ('discommensurations') on $(10\bar{1}2)$ TMA-ZC.

We are indebted to A. Janner and M. Elwenspoek for their critical reading of the manuscript.

References

ALMAIRAC, R., RIBET, M., RIBET, J. W. & BZIOUET, M. (1980). *J. Phys. Lett.* **41**, L315-L318.

CABRERA, N. & LEVINE, M. M. (1956). *Philos. Mag.* **1**, 450-471.

DAM, B. (1985). *Phys. Rev. Lett.* **55**, 2806-2809.

DAM, B. & JANNER, A. (1983). *Z. Kristallogr.* **165**, 247-254.

DAM, B. & JANNER, A. (1986). *Acta Cryst.* B**42**, 69-77.

DAM, B., POLMAN, E. & VAN ENCKEVORT, W. J. P. (1984). In *Industrial Crystallization* 1984, edited by S. J. JANCIC & E. J. DE JONG, pp. 97-102. Amsterdam: North-Holland.

DAM, B. & VAN ENCKEVORT, W. J. P. (1984). *J. Cryst. Growth* **69**, 306-316.

DEHLINGER, U. (1927). *Z. Kristallogr.* **65**, 615-623.

EERDEN, J. P. VAN DER, BENNEMA, P. & CHEREPANOVA, T. A. (1978). *Prog. Cryst. Growth Charact.* **1**, 219-254.

ENCKEVORT, W. J. P. VAN (1984). *Prog. Cryst. Growth Charact.* **9**, 1-49.

ENCKEVORT, W. J. P. VAN & ODEKERKEN, J. (1982). Thesis, Univ. of Nijmegen.

HARTMAN, P. (1973). In *Crystal Growth: An Introduction*, edited by P. HARTMAN, pp. 367-402. Amsterdam: North-Holland.

HOEK, B. VAN DER, VAN DER EERDEN, J. P. & BENNEMA, P. (1982). *J. Cryst. Growth* **56**, 621-632.

HOEK, B. VAN DER, VAN DER EERDEN, J. P., BENNEMA, P. & SUNAGAWA, I. (1982). *J. Cryst. Growth* **58**, 365-380.

HOGERVORST, A. C. R. (1983). *Conference Proceedings. Int. Conf. on Phase Transformations in Solids.*

JANNER, A. (1983). *Symmetries and Properties of Non-Rigid Molecules: A Comprehensive Survey*, edited by J. MARNANI & J. SERRE. *Studies in Physical and Theoretical Chemistry*, Vol. 23, pp. 461-486. Amsterdam: Elsevier.

JANNER, A. & JANSSEN, T. (1980). *Acta Cryst.* A**36**, 399-408, 408-415.

JANNER, A., RASING, TH., BENNEMA, P. & VAN DER LINDEN, W. H. (1980). *Phys. Rev. Lett.* **45**, 1700-1702.

JETTEN, L. A. M. J., VAN DER HOEK, B. & VAN ENCKEVORT, W. J. P. (1983). *J. Cryst. Growth*, **62**, 603-611.

LANDAU, L. D. (1965). In *Collected Papers of L. D. Landau*, edited by D. TER HAAR, pp. 540-545. Oxford: Pergamon Press.

MCMILLAN, W. L. (1976). *Phys. Rev. B*, **14**, 1496-1502.

MARION, G., ALMAIRAC, R., LEFEBVRE, J. & RIBET, M. (1981). *J. Phys. C*, **14**, 3177-3185.

MASHIYAMA, H., HASEBE, K. & TANISAKI, S. (1980). *J. Phys. Soc. Jpn*, B**49**, 92-94.

MASHIYAMA, H., TANISAKI, S. & HAMANO, K. (1982). *J. Phys. Soc. Jpn*, **51**, 2538-2544.

MÖNCH, W. (1979). *Surf. Sci.* **86**, 672-699.

PATER, C. J. DE & VAN DIJK, C. (1978). *Phys. Rev. B*, **18**, 1281-1293.

RIBET, M. (1983). *J. Phys. Lett.* **44**, L963-L969.

RIJPKEMA, J. J. M., KNOPS, H. F. J., BENNEMA, P. & VAN DER EERDEN, J. P. (1982). *J. Cryst. Growth*, **61**, 295-306.

ROTTMAN, C. & WORTIS, M. (1984). *Phys. Rep.* **103**, 59-79.

SAWADA, S., SHIROISHI, Y., YAMAMOTO, A., TAKASHIGE, M. & MATSUO, M. (1977). *J. Phys. Soc. Jpn*, **43**, 2099-2100.

SCHULZ, H. J. (1985). *J. Phys.* **46**, 257-269.

TANISAKI, S. & MASHIYAMA, H. (1980). *J. Phys. Soc. Jpn Lett.* **48**, 339-340.

TSUKAMOTO, K. (1983). *J. Cryst. Growth*, **61**, 199-204.

TSUKAMOTO, K. & SUNAGAWA, I. (1985). *J. Cryst. Growth*, **71**, 183-190.

WEEKS, J. D. & GILMER, G. H. (1979). In *Advances in Chemical Physics*, Vol. XL, edited by I. PRIGOGINE & S. A. RICE, pp. 157-174.

WOLFF, P. M. DE (1977). *Acta Cryst.* A**33**, 493-497.

WOLFF, P. M. DE, JANSSEN, T. & JANNER, A. (1981). *Acta Cryst.* A**37**, 625-636.

Acta Cryst. (1987). B**43**, 71-75

Comparative Study of the Crystal Structures of Isotypic $MX_2.H_2O$, M = Sr, Ba, and X = Cl, Br, I. Bifurcated H Bonds in Solid Hydrates

BY H. D. LUTZ, W. BUCHMEIER AND B. ENGELEN

Laboratorium für Anorganische Chemie, Universität-GH-Siegen, D-5900 Siegen, Federal Republic of Germany

(*Received* 10 *February* 1986; *accepted* 4 *August* 1986)

Abstract

$SrCl_2.H_2O$: $M_r = 176{\cdot}54$, $a = 10{\cdot}881\ (1)$, $b = 4{\cdot}162\ (1)$, $c = 8{\cdot}864\ (1)$ Å, $V = 401{\cdot}4\ (1)$ Å^3, $D_x = 2{\cdot}921$ Mg m^{-3}, $\mu = 14{\cdot}16$ mm^{-1}, $F(000) = 328$, $R = 0{\cdot}025$ for 1103 unique reflections; $SrBr_2.H_2O$: $M_r = 265{\cdot}46$, $a = 11{\cdot}464\ (1)$, $b = 4{\cdot}295\ (1)$, $c = 9{\cdot}229\ (1)$ Å, $V = 454{\cdot}4\ (1)$ Å^3, $D_x = 3{\cdot}880$ Mg m^{-3}, $\mu = 28{\cdot}75$ mm^{-1}, $F(000) = 472$, $R = 0{\cdot}060$ for 763 reflections; $SrI_2.H_2O$: $M_r = 359{\cdot}44$, $a = 12{\cdot}474\ (2)$, $b = 4{\cdot}495\ (1)$, $c = 9{\cdot}741\ (2)$ Å, $V = 546{\cdot}2\ (1)$ Å^3, $D_x = 4{\cdot}370$ Mg m^{-3}, $\mu = 20{\cdot}62$ mm^{-1}, $F(000) = 616$, $R = 0{\cdot}043$ for 966 reflections; $BaCl_2.H_2O$: $M_r = 226{\cdot}26$, $a = 11{\cdot}094\ (1)$, $b = 4{\cdot}500\ (1)$, $c = 9{\cdot}054\ (1)$ Å, $V = 452{\cdot}0\ (1)$ Å^3, $D_x = 3{\cdot}324$ Mg m^{-3}, $\mu = 9{\cdot}79$ mm^{-1}, $F(000) = 400$, $R = 0{\cdot}021$ for 1231 reflections; $BaBr_2.H_2O$: $M_r = 315{\cdot}18$, $a = 11{\cdot}643\ (2)$, $b = 4{\cdot}604\ (1)$, $c = 9{\cdot}438\ (2)$ Å, $V = 505{\cdot}9\ (1)$ Å^3, $D_x = 4{\cdot}137$ Mg m^{-3}, $\mu = 23{\cdot}34$ mm^{-1}, $F(000) = 544$, $R = 0{\cdot}040$ for 1098 reflections; $BaI_2.H_2O$: $M_r = 409{\cdot}16$, $a = 12{\cdot}494\ (1)$, $b = 4{\cdot}772\ (1)$, $c = 10{\cdot}014\ (1)$ Å, $V = 597{\cdot}1\ (1)$ Å^3, $D_x = 4{\cdot}551$ Mg m^{-3}, $\mu = 16{\cdot}75$ mm^{-1}, $F(000) = 688$, $R = 0{\cdot}023$ for 935 reflections; all orthorhombic, *Pnma* (D_{2h}^{16}), $Z = 4$, Mo $K\alpha$, $\lambda = 0{\cdot}71069$ Å and $T = 293$ K. The structures consist of distorted face-sharing $MX_7(H_2O)_2$ tricapped trigonal prisms forming columns and channels along [010]. The distortion of the water molecules, which form weak,

0108-7681/87/010071-05$01.50